Absence of the peroxiredoxin Pmp20 causes peroxisomal protein leakage and necrotic cell death

Aksam, Eda Bener; Jungwirth, Helmut; Kohlwein, Sepp D.; Ring, Julia; Madeo, Frank; Veenhuis, Marten; van der Klei, Ida J.

Published in:
Free Radical Biology and Medicine

DOI:
10.1016/j.freeradbiomed.2008.07.010

Free Radical Biology & Medicine 45 (2008) 1115–1124

Contents lists available at ScienceDirect

Free Radical Biology & Medicine

journal homepage: www.elsevier.com/locate/freeradbiomed

Original Contribution

Absence of the peroxiredoxin Pmp20 causes peroxisomal protein leakage and necrotic cell death

Eda Bener Aksam [a], Helmut Jungwirth [b], Sepp D. Kohlwein [b], Julia Ring [b], Frank Madeo [b], Marten Veenhuis [a,c], Ida J. van der Klei [a,c,*]

[a] Molecular Cell Biology, Groningen Biomolecular Sciences and Biotechnology Institute, University of Groningen, Haren, The Netherlands
[b] Institute of Molecular Biosciences, University of Graz, 8010 Graz, Austria
[c] Kluyver Centre for Genomics of Industrial Fermentation, Julianalaan 67, 2628 BC Delft, The Netherlands

ARTICLE INFO

Article history:
Received 8 May 2008
Revised 1 July 2008
Accepted 8 July 2008
Available online 25 July 2008

Keywords:
Peroxisome
ROS
Peroxiredoxin
Cell death

ABSTRACT

We analyzed the role of the peroxisomal peroxiredoxin Pmp20 of the yeast *Hansenula polymorpha*. Cells of a *PMP20* disruption strain (*pmp20*) grew normally on substrates that are not metabolized by peroxisomal enzymes, but showed a severe growth defect on methanol, the metabolism of which involves a hydrogen peroxide producing peroxisomal oxidase. This growth defect was paralleled by leakage of peroxisomal matrix proteins into the cytosol. Methanol-induced *pmp20* cells accumulated enhanced levels of reactive oxygen species and lipid peroxidation products. Moreover, the fatty acid composition of methanol-induced *pmp20* cells differed relative to WT controls, suggesting an effect on fatty acid homeostasis. Plating assays and FACS-based analysis of cell death markers revealed that *pmp20* cells show loss of clonogenic efficiency and membrane integrity, when cultured on methanol. We conclude that the absence of the peroxisomal peroxiredoxin leads to loss of peroxisome membrane integrity and necrotic cell death.

Introduction

In biological systems the harmful effects of reactive oxygen species (ROS) are the cause of oxidative stress, which has been implicated in many human diseases and in ageing [1]. In eukaryotic cells mitochondria are considered to be the prime sources of ROS, which are generated as by-products of normal mitochondrial oxidative metabolism. However, peroxisomal oxidases produce hydrogen peroxide (H_2O_2) and hence may also contribute to intracellular ROS levels. Although H_2O_2 has no unpaired electrons and thus is not a radical, it is also often qualified as ROS because it can easily convert into the highly reactive hydroxyl radical (•OH) by transition metal ion decomposition. Transition metal ions, like iron and copper, are present in peroxisomes, where they are generally in complex with peroxisomal enzymes (e.g., as a cofactor or in heme). However, under certain conditions these metal ions can be released from the peroxisomal enzyme [2].

Catalase (CAT) is a well-known peroxisomal marker enzyme that decomposes H_2O_2 into water and molecular oxygen. Compartmentalization of H_2O_2 producing oxidases together with CAT in peroxisomes is assumed to prevent release of H_2O_2 from the organelle into the cytosol. This colocalization is especially important because CAT has a relatively low affinity for H_2O_2 (K_m of approx. 25 mM) [3,4]. The importance of CAT as peroxisomal antioxidant enzyme is well established [2,5,6]. However, peroxisomes also contain other antioxidant enzymes, among others peroxiredoxins (Prxs). As yet, the physiological significance of peroxisomal Prxs is still largely speculative.

Prxs are thiol-specific antioxidant enzymes, which are present in organisms from all kingdoms. They are involved in the enzymatic degradation of H_2O_2 and organic hydroperoxides (ROOH). All Prxs contain one or more conserved cysteine (Cys) residues that undergo a cycle of peroxide-dependent oxidation and thiol-dependent reduction. In eukaryotic cells, Prx enzymes have been localized to different cell compartments including the cytosol, the endoplasmic reticulum, mitochondria, peroxisomes, and nuclei [7,8].

The first peroxisomal Prx was described in the yeast *Candida boidinii*. It was designated CbPmp20 because it was initially identified as a *p*eroxisomal *m*embrane *p*rotein, hence its name [9]. However, later studies revealed that it is a peroxisomal matrix-localized protein,

Abbreviations: ABTS, 2,2-azino-di-[2-ethylbenztioazolin sulfonate]; AMO, amine oxidase; AO, alcohol oxidase; CAT, catalase; GFP-SKL, green fluorescent protein with a C-terminal peroxisomal targeting sequence (serine-lysine-leucine); H_2DCFDA, dichlorodihydrofluorescein diacetate; MDA, malondialdehyde; PTS1, peroxisomal targeting signal 1; ROS, reactive oxygen species; TBA, thiobarbituric acid; TBARS, thiobarbituric acid-reactive species; URA3, gene encoding orotidine-5′-phosphate (transformation selection marker for uracil auxotrophy); YCA1, yeast caspase 1; YND, 0.67% yeast nitrogen base without amino acids supplemented with 1% glucose; YPD, 1% yeast extract, 1% peptone, 1% glucose.

* Corresponding author. Molecular Cell Biology, Groningen Biomolecular Sciences and Biotechnology Institute; P.O. Box 14; Haren 9750 AA, The Netherlands. Fax: +31 50 363 8280.
E-mail address: I.J.van.der.Klei@rug.nl (I.J. van der Klei).

0891-5849/$ – see front matter © 2008 Elsevier Inc. All rights reserved.
doi:10.1016/j.freeradbiomed.2008.07.010

which may associate to the inner surface of the peroxisomal membrane [10]. In vitro, CbPmp20 has glutathione peroxidase activity toward alkyl hydroperoxides and H_2O_2 [3].

Mammalian cells have six Prxs, designated peroxiredoxin 1–6. The mammalian homologue of CbPmp20 is peroxiredoxin 5. Like CbPmp20 this protein is localized to peroxisomes and contains a C-terminal peroxisomal targeting signal 1 (PTS1) [11]. However, the N-terminus of mammalian peroxiredoxin 5 contains mitochondrial targeting information and localization studies suggest that the protein may be localized to both peroxisomes and mitochondria [12]. Human PMP20 is expressed in all tissues and upregulated in human osteoarthritis [13] and in Graves' thyroid [14], indicating an important physiological role of PMP20 in man.

In order to further study the physiological function of Pmp20 in vivo, we identified the Pmp20 homologue of the yeast *Hansenula polymorpha* and analyzed the properties of a *PMP20* disruption strain (*pmp20*). The rational behind this approach is that *H. polymorpha* can grow on methanol as sole source of carbon and energy, a compound that is oxidized by a peroxisomal alcohol oxidase (AO). AO-mediated oxidation of methanol results in the generation of formaldehyde and H_2O_2. Hence, during growth of cells on methanol, vast amounts of H_2O_2 are produced (one molecule for each methanol molecule oxidized). This renders this organism very attractive to study the physiological role of peroxisomal antioxidant enzymes [6]. Here we present evidence that peroxiredoxin Pmp20 protects peroxisomal membranes and prevents necrotic cell death.

Materials and methods

Organisms and growth

The *H. polymorpha* strains used in this study are shown in Table S1. Yeast cells were grown as described before [15] at 37 °C in batch cultures in mineral medium containing 0.25% ammonium sulfate or 0.25% methylamine as nitrogen source supplemented with 0.25% glucose or 0.5% methanol as carbon sources. Amino acids were added to a final concentration of 30 mg/L as required. To test whether GFP-SKL (green fluorescent protein with a C-terminal peroxisomal targeting sequence [serine-lysine-leucine]) leaked from peroxisomes, cells producing GFP-SKL under control of the amine oxidase promoter (P_{AMO}) were extensively precultivated on medium containing glucose as carbon source and methylamine as nitrogen source. The P_{AMO} was subsequently repressed by shifting the cells to a medium containing ammonium sulfate without carbon source and incubation for 30 min to deplete the cells from GFP-SKL mRNAs [16]. Subsequently, methanol was added to allow growth and to induce peroxisomes.

For analysis of import of GFP-SKL into peroxisomes, cells were pregrown on glucose/ammonium sulfate medium and then shifted to media containing methanol/ methylamine to induce peroxisome proliferation and P_{AMO}.

Molecular techniques

Standard recombinant DNA techniques [17] and transformation of *H. polymorpha* [18] were performed as detailed before.

Construction of an H. polymorpha PMP20 disruption strain

A *PMP20* disruption cassette was constructed in which the ATG start codon was replaced by the stop codon TAA. The Invitrogen MultiSite Gateway System was used to construct an *URA3* containing disruption cassette. PCR primers (Table S2) containing attB recombination sides were used for amplification of the 5′- and 3′-flanking regions of *PMP20* and as well as the *H. polymorpha URA3* gene [19]. In the "5′-rev-pmp20" primer the ATG start codon was replaced by the TAA. After recombination in *Escherichia coli* to obtain the 5′-entry vector pEBA017, the 3′-entry vector pEBA018, and the pENT221_ura3 containing *URA3*, the complete disruption cassette was obtained and designated as pEBA019. The disruption cassette was amplified by PCR using primers "cut-fwd-pmp20" and "cut-rev-pmp20." The presence of the introduced stop codon was confirmed by sequencing of the PCR product. The resulting disruption cassette was transformed into electro-competent *H. polymorpha* wild-type *leu1.1 ura3*. After transformation Ura^+ clones were selected on leucine containing YND plates (0.67% yeast nitrogen base without amino acids supplemented with 1% glucose and 2% agar). Replacement of the *PMP20* gene by the disruption cassette in the genome at the correct position was confirmed by Southern blot analysis.

Construction of H. polymorpha yca1 and pmp20yca1 strains

A *YCA1* (gene encoding yeast caspase 1) disruption cassette was constructed in which the ATG start codon was replaced by the stop codon TAA. Two-step cloning was used to construct the plasmid pEBA031 which contains the disruption cassette. PCR primer couples shown in Table S2 were used for amplification of the 5′- and 3′-flanking regions of *YCA1* from *H. polymorpha* genomic DNA. The amplified fragments were cloned to pFEM39 in the upstream and downstream flanking regions of the Zeocine marker gene. The disruption cassette was obtained by PCR using primers "pcr-yca1-fw" and "pcr-yca1-rev." The resulting disruption cassette was transformed separately into electro-competent *H. polymorpha* wild-type *leu1.1* and *pmp20 leu1.1* cells. After transformation Zeocine-resistant clones were selected on YPD plates (1% yeast extract, 1% peptone, 1% glucose, and 2% agar) containing zeocine. Replacement of the *YCA1* gene by the disruption cassette in the genome at the correct position was confirmed by Southern blot analysis in both strains.

Construction of a pmp20::P_{AMO}GFP-SKL strain

The PHIPX5-GFP-SKL plasmid [20] containing the GFP-SKL gene under the control of *H. polymorpha* P_{AMO} was linearized with *Bsi*WI and transformed to *H. polymorpha pmp20* cells. After transformation Leu^+ clones were selected on YND plates. Correct integration and the copy number of the integrated gene were confirmed by Southern blot analysis.

Construction of plasmid pEBA025 (P_{AMO}His6-PMP20) and complementation of pmp20

Using PCR, six copies of the histidine coding triplet were introduced after the ATG start codon of *PMP20*, resulting in a gene encoding HpPmp20 containing a His_6 tag at the extreme N-terminus. A *Bam*HI restriction site was included in the primer "his-pmp20-fwd" that was used to amplify the *PMP20* gene with the reverse primer "his-pmp20-rev" (Table S2). The amplified fragment was digested with *Bam*HI and ligated with the *Sma*I/*Bam*HI-digested PHIPX5-GFP-SKL plasmid, containing leucine as a marker. The resulting plasmid, designated pEBA025 containing *His6-PMP20* under control of the P_{AMO}, was transformed to cells of the *pmp20* strain.

Biochemical methods and microscopy

Preparation of crude extracts, measurement of protein concentrations, Western blotting, cell fractionation, and enzyme activity measurements were performed as described before [21–23]. The colorimetric AO activity assay is an indirect method based on the methanol-dependent production of H_2O_2. The H_2O_2 produced oxidizes ABTS (2,2-azino-di-[2-ethylbenztioazolin sulfonate]), a reaction catalyzed by horseradish peroxidase. The rate of oxidized ABTS formation is spectrophotometrically monitored at 340 nm. Catalase activity is directly measured by spectrophotometrically monitoring the decrease in H_2O_2 concentration at 240 nm. Cytochrome *c* oxidase is determined by monitoring the decrease in reduced cytochrome *c* at 550 nm.

Western blots were probed with specific polyclonal antibodies against various *H. polymorpha* proteins. Antibodies against *H.*

polymorpha proteins were generated in rabbit as described previously for AO, CAT, Pex5p, Pex10p, Pex14p, and Pyc1p [24–29], respectively. The anti-*H. polymorpha* Pex11p antiserum was raised in rabbit using two synthetic Pex11p peptides (J.A.K.W. Kiel, unpublished results). Protein carbonylation was analyzed using the Oxy-blot kit (Chemicon, USA). Electron microscopy was performed as described [23] and fluorescence microscopy was performed on a Zeiss Axioskop50 fluorescence microscope. Images were taken with a Princeton Instruments 1300Y digital camera. GFP signal was visualized with a 470/40-nm bandpass excitation filter, a 495-nm dichromatic mirror, and a 525/50-nm bandpass emission filter.

Purification of Pmp20 and generation of Pmp20 antiserum

His_6-Pmp20 was produced in *H. polymorpha pmp20* cells containing plasmid pEBA025. The protein was purified from a total membrane fraction, solubilized in a buffer containing 50 mM Tris-HCl, pH 7.5, and 1% SDS, using Nickel-NTA beads (Qiagen) as described by the manufacturer. Fractions containing one major protein band of the expected molecular weight (~20 kDa), which was recognized by anti-His_6 antibodies, were selected. The 20-kDa protein band was cut from the gel and used for immunization of rabbits.

Analysis of intracellular ROS levels

Reactive oxygen species were visualized using the ROS-specific fluorescent dye dichlorodihydrofluorescein diacetate (H_2DCFDA) [30] and quantified using a fluorescence activated cell sorter (FACS; Coulter Epics Elite equipped with a Gated Amplifier, Coulter Electronics, FL). The experiments were performed with two independent cultures and each measurement was performed in triplicate.

Lipid peroxidation analysis

Lipid peroxidation was quantified by determination of thiobarbituric acid (TBA)-reactive substances (TBARS) [31]. Cells were collected by centrifugation, washed once with demineralized water, and resuspended to a density of 100 OD_{600} units/ml in ice-cold 50 mM potassium phosphate buffer, pH 7.2, containing protease inhibitors. Cells were broken with glass beads and 500 µl of the cell extract was used per assay. One milliliter of TBA reagent was added and the mixture was incubated at 90 °C for 20 min. After cooling on ice, samples were centrifuged at 20,800 *g* for 5 min. The absorbance of the samples was measured at 535 nm against a reference solution in which the cell extract was replaced by buffer. The TBARS concentration was expressed as picomole malondialdehyde per milligram protein.

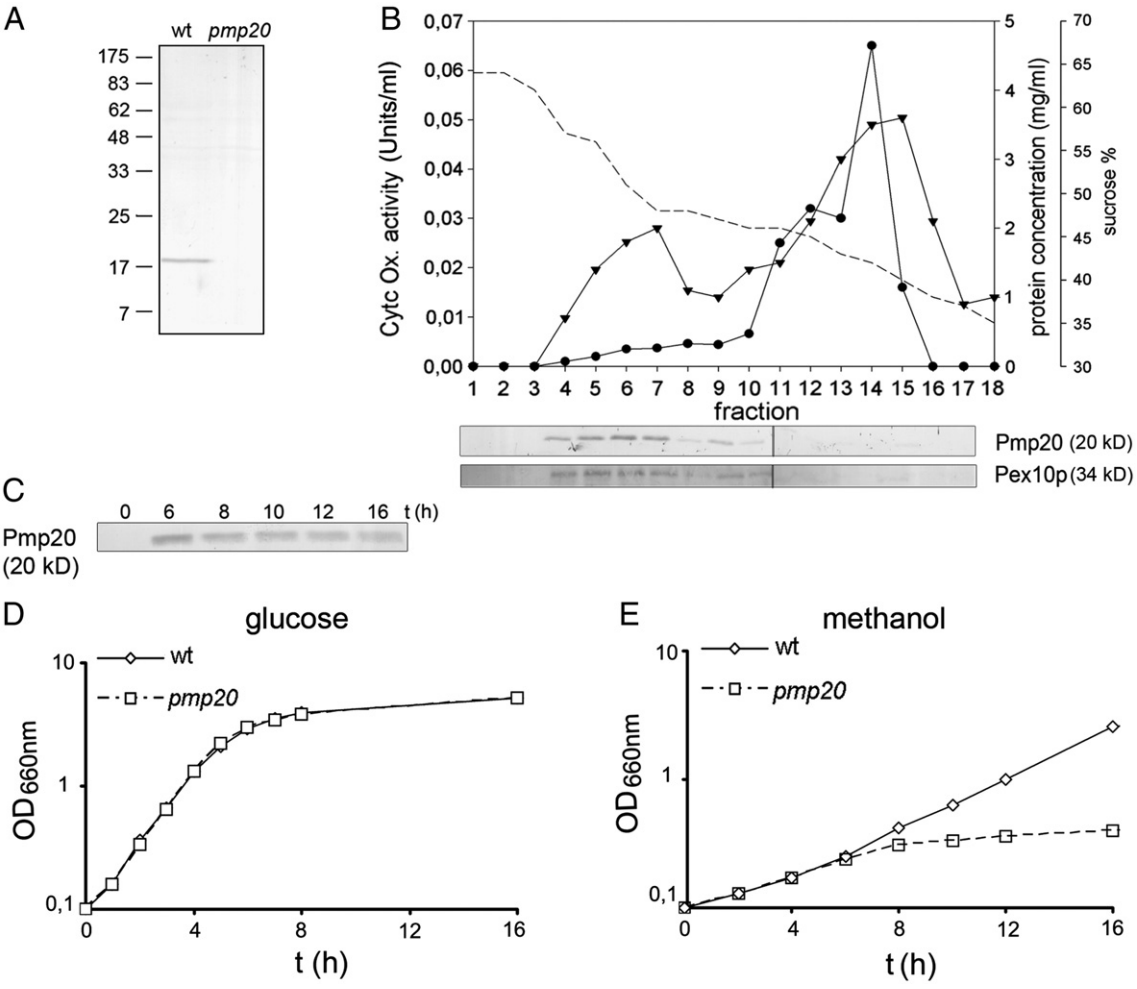

Fig. 1. Identification of HpPmp20 and physiological properties of *pmp20* cells. (A) Western blot prepared from crude extracts of methanol-grown WT and *pmp20* cells, showing the specificity of the polyclonal anti-Pmp20 antiserum. (B) Sucrose density gradient prepared of homogenized methanol-grown *H. polymorpha* WT cells. In the protein peak at approximately 50% sucrose Pmp20 cosediments with the peroxisomal membrane protein Pex10p, indicating the peroxisomal nature of Pmp20. The symbols on the graph indicate: (▾) protein concentration in mg/ml, (—) sucrose concentration (%), (●) cytochrome *c* oxidase activity (Units/ml). (C) Induction profile of Pmp20 protein at various time points after a shift of cells from glucose (t=0 h) to methanol. On glucose Pmp20 is below the limit of detection but readily induced during adaptation of cells to methanol. (D,E) *pmp20* cells grow normally on glucose like WT, but show a severe growth defect on methanol, initiating after 8 h of cultivation on methanol.

Lipid extraction and analysis

Lipids from *H. polymorpha* cells were extracted by the method of Folch essentially as described [32]. In brief, 10^9 cells were harvested by centrifugation, washed in ice-cold distilled water, and transferred into cooled homogenization tubes, in 5 ml ice-cold methanol. Cells were homogenized in a Braun Melsungen homogenizer under CO_2 cooling. Lipids were extracted with 10 ml $CHCl_3$ for 1 h. After addition of 3 ml 0.034% $MgCl_2$ solution, cell slurry and glass beads are transferred to centrifugation tubes; the homogenization tubes are rinsed with 5 ml $CHCl_3$/methanol 2/1 (v/v), and 1 ml 0.034% is added to the homogenate. Phase separation occurs by centrifugation at 2500 rpm for 2–5 min. The lower phase is reextracted with 5 ml $CHCl_3$/methanol/H_2O 3/48/47 per volume and cleared by centrifugation (2 min at 2500 rpm). The lower phase is dried in a rotavapor and residual water removed azeotropically by addition of 3 ml toluene/ethanol (4/3 v/v). Lipid extracts are stored in $CHCl_3$/methanol (2/1, v/v) at –20 °C. Fatty acid methylesters (FAMEs) are prepared from lipid extracts of ~2 10^8 cells. Extracts are dried under a stream of nitrogen, and dissolved in 0.5 ml benzene. After addition of 2 ml 14% BF_3 in methanol, samples are heated to 100 °C for 45 min. After cooling on ice, 1 ml of distilled H_2O is added and FAMEs are extracted three times with 3 ml petrol ether (PE) each. The collected PE phases are dried under a stream of nitrogen and FAMEs are dissolved in 200–300 l of PE.

GC-MS analysis of fatty acid methylesters

GC-MS analysis of the fatty acid methyl esters was done on a Trace-GC Ultra-DSQ MS spectrometer (ThermoElectron, Waltham, MA) using an HP-5MS separation column (30 m, i.d. 0.25 mm). Samples were dissolved in 200 ml petrol ether and 1 ml was injected in splitless mode, with 1 ml/min He carrier gas flow. The temperature gradient started at 60 °C (hold time 4 min) and increased up to 300 °C (20°C/min, hold time 10 min). MS analysis was performed in positive EI mode (electron energy 70 EV, mass range 50–800 *m/z*). Quantification of signals was performed with Xcalibur 1.4 software (ThermoElectron, Waltham, MA).

Survival plating and tests for apoptotic and necrotic markers

For survival platings, cell cultures were diluted, cell concentration was determined with a CASY cell counter, and aliquots containing 500 cells were plated on YPD plates. The number of colonies was determined after 1 day at 37 °C.

Annexin V/PI-costaining with modifications in the protoplasting step were performed and quantified using FACSAria as described [33]. Protoplasting of *H. polymorpha* was done as described before [21].

Results

Identification of a peroxisomal peroxiredoxin in H. polymorpha

A search in the *Hansenula polymorpha* genome database [34] revealed the presence of a gene (NCBI GenBank Accession Number EU200440) encoding a protein that is homologous (63% identity) to the peroxisomal Prx of *C. boidinii,* CbPmp20 [3]. Like CbPmp20, the putative *H. polymorpha* homologue, HpPmp20, is a 1-Cys type Prx with a C-terminal –AKL sequence, which represents a peroxisomal targeting signal type 1.

An antiserum generated against HpPmp20 specifically recognized a protein band of 20 kDa which is the expected molecular mass based on its amino acid composition (Fig. 1A). This band was absent in

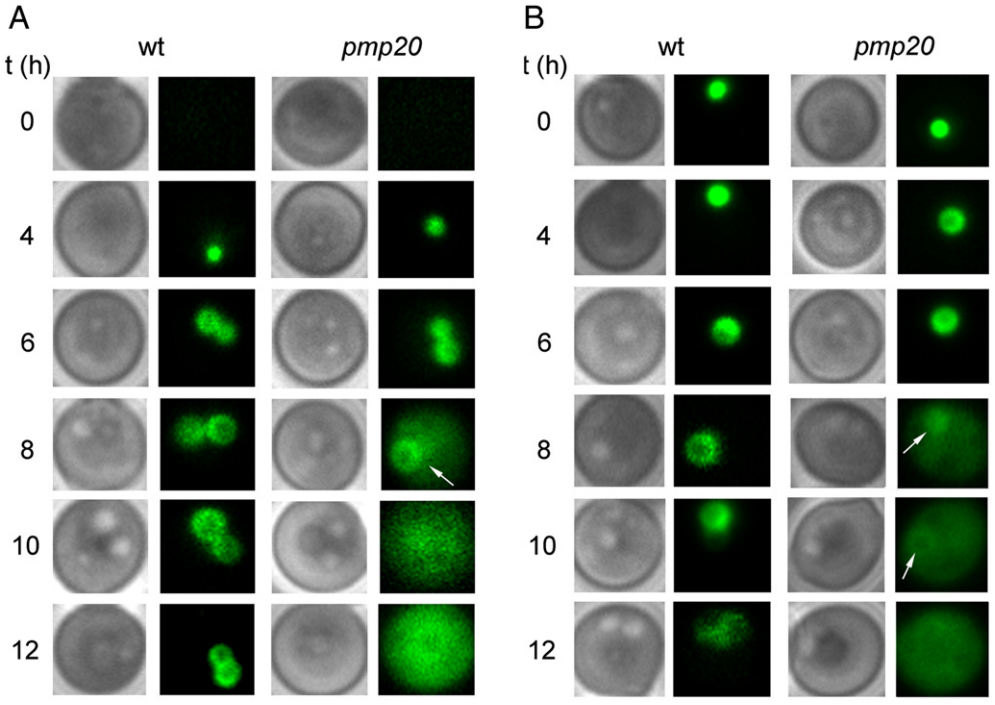

Fig. 2. Fluorescence microscopy analysis of *pmp20* and WT cells. Cells produce GFP-SKL from the methylamine-inducible amine oxidase promoter. (A) Cells are shifted from glucose/ammonium sulfate (t=0 h) to methanol/methylamine-containing media and analyzed at various time points after the shift. On glucose/ammonium sulfate, GFP fluorescence was undetectable but became induced after the shift to methanol/methylamine. In *pmp20* cells, GFP fluorescence was confined to distinct spots, representing peroxisomes (t=4, 6 h) but also appeared in the cytosol initiating 8 h after the shift (peroxisome indicated by arrow). At later time points (t=10, 12 h) peroxisomes were no longer detectable and GFP fluorescence was distributed over the cytosol. In WT controls peroxisome development was normal. Panel B represents the fate of peroxisomal GFP-SKL present in glucose/methylamine-grown cells (t=0 h) after a shift of cells to methanol/ammonium sulfate, conditions that induce peroxisome biogenesis (by methanol) in conjunction with full repression of GFP-SKL synthesis (by ammonium sulfate). In the initial stage of growth (t=4, 6 h) the GFP spot enlarges, indicative for growth of peroxisomes on methanol. At 8 h of cultivation also cytosolic GFP is observed (peroxisome indicated by arrow) but the organelles are no longer observed after 12 h of cultivation. In WT controls GFP fluorescence is confined to peroxisomes.

extracts prepared from cells of a *PMP20* disruption strain (*pmp20*; Fig. 1A); hence the antiserum was considered a bona fide HpPmp20 antiserum. Western blot analysis using these antibodies and fractions of a sucrose density gradient prepared from a homogenate of methanol-grown *H. polymorpha* WT cells revealed that HpPmp20 cosedimented with the peroxisomal membrane protein HpPex10p, confirming its peroxisomal localization (Fig. 1B). Further analysis showed that HpPmp20p is below the level of detection in glucose-grown cells, but induced during growth of cells on methanol (Fig. 1C), suggesting a function during methylotrophic growth conditions. This was corroborated by the observation that *pmp20* cells displayed aberrant growth on methanol, but not on glucose (Figs. 1D and E). Growth of *pmp20* cells was also normal on ethanol or glycerol (data not shown), two carbons sources that are not metabolized via peroxisomal oxidases (data not shown). The aberrant growth phenotype on methanol was restored by reintroducing the *H. polymorpha PMP20* gene, confirming that this phenotype was caused by disruption of the *PMP20* gene (data not shown).

Peroxisomes in pmp20 cells become leaky for proteins

On shifting *pmp20* cells from peroxisome repressing conditions (glucose/ammonium sulfate) to conditions that induce the formation of peroxisomes and synthesis of the fluorescent peroxisomal marker protein GFP-SKL (methanol/methylamine), peroxisomes (Fig. 2A) and the key enzymes of methanol metabolism, alcohol oxidase (AO) and CAT (Fig. 3A), are normally induced and enzymatically active (Figs. 3B and C). However, after 8 h of incubation GFP fluorescence was also detectable in the cytosol of *pmp20* cells, the intensity of which increased after prolonged cultivation (Fig. 2A). Since GFP-SKL is produced from the inducible amine oxidase promoter (P_{AMO}), we analyzed whether the cytosolic GFP-SKL protein in *pmp20* cells was related to leakage from peroxisomes or due to a failure in protein import. To this end, cells were pregrown on glucose/methylamine to induce P_{AMO} and thus GFP-SKL synthesis to visualize peroxisomes in the glucose inoculum cells (Fig. 2B). Subsequently, the cells were placed in fresh methanol/ammonium sulfate medium to induce peroxisome formation (by methanol) in conjunction with full repression of P_{AMO} (by ammonium sulfate). The data (Fig. 2B) show that in *pmp20* cells peroxisomes initially normally increase in size as in WT. However, after 8 h of cultivation on methanol/ammonium sulfate the first GFP fluorescence was also observed in the cytosol, suggesting that this protein resulted from leakage from the organelles. At 12 h of cultivation the organelles could no longer be observed and cytosolic fluorescence was prominent. In WT controls GFP-SKL remained confined to spots that slowly reduced in intensity at later stages of cultivation (Fig. 2B). We interpret this that in WT the originally present GFP-SKL is diluted out over newly formed organelles during vegetative cell multiplication.

Electron microscopy analyses, however, revealed that virtually intact peroxisomes are present in *pmp20* cells, indistinguishable from WT organelles, at all time points examined (up to 16 h) after the shift of cells from glucose to methanol (compare Figs. 4A–D). We never observed organelles having damaged membranes or subject to selective degradation by pexophagy (data not shown). Immunolabeling

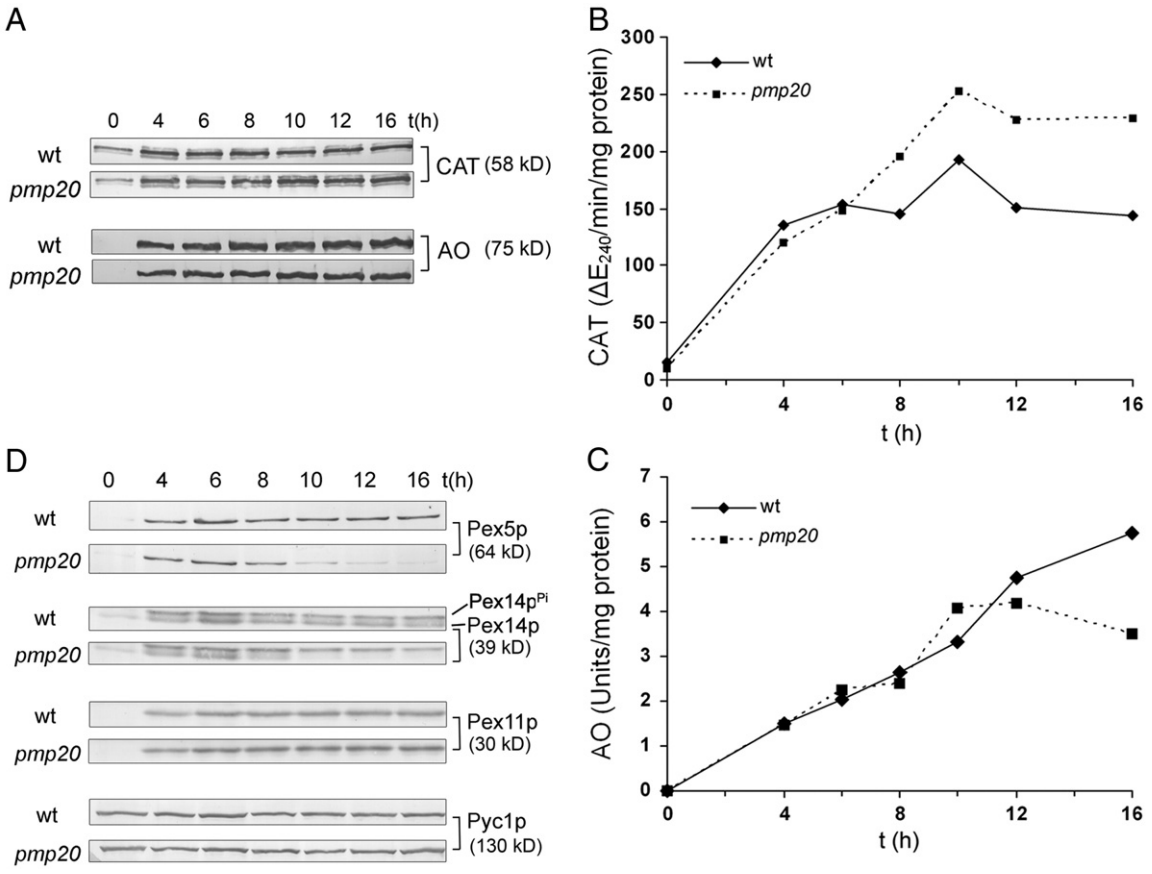

Fig. 3. Induction and activities of peroxisomal enzymes in *pmp20* cells. Panel A shows that the synthesis of the key enzymes of methanol metabolism, alcohol oxidase (AO) and catalase (CAT), is induced after a shift of cells from glucose (t=0 h) to methanol. During induction on methanol the levels of CAT are enhanced in *pmp20* cells relative to those of WT controls. By contrast, AO protein is highest in WT cells. The proteins levels are reflected in the patterns of specific CAT (B) and AO (C) enzyme activities in the two strains. Panel D shows the induction patterns of Pex5p and Pex14p. The blots show the strong reduction in Pex5p levels, relative to WT, initiating after 8 h of cultivation on methanol. At this time point also the nonphosphorylated form of Pex14p (lower band of the Pex14p doublet evident at t=6 h) rapidly declines and is undetectable in samples taken at 16 h on methanol. Under these conditions the peroxisomal membrane protein Pex11p remains normally present, similar as pyruvate carboxylase (Pyc1p), taken as cytosolic control.

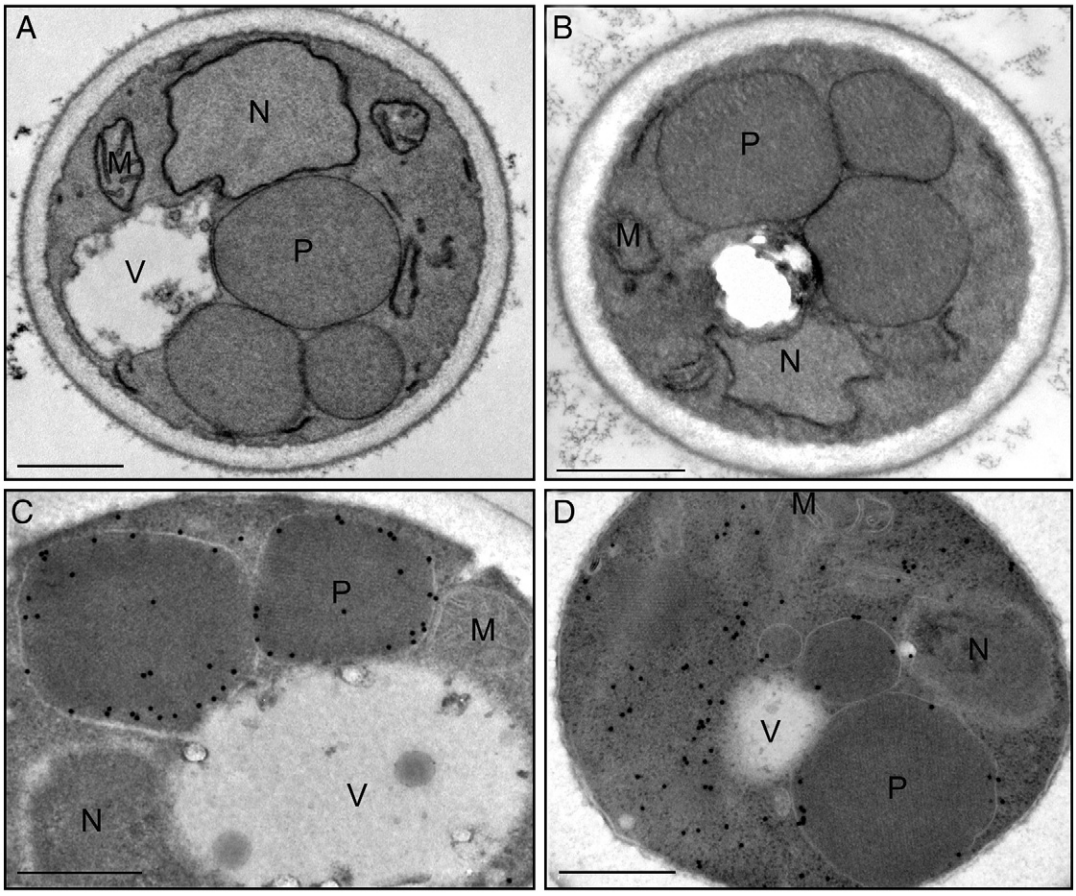

Fig. 4. Peroxisomes normally develop in *pmp20* cells. Panels A and B show characteristic surveys of ultrathin sections of $KMnO_4$-fixed cells, grown for 16 h on methanol. Peroxisome development in *pmp20* cells (B,D) is indistinguishable from that in WT (A,C) controls. Also, disintegration of peroxisomal membranes is never detected. Immunocytochemical analysis of catalase protein shows that anti-catalase-specific labeling in *pmp20* cells is predominantly observed in the cytosol (D), but characteristically present at the edge of the peroxisomes in WT cells (C).

experiments revealed that the bulk of the peroxisomal catalase (Fig. 4D) as well as low amounts of AO protein (not shown) was mislocalized to the cytosol in *pmp20* cells, but not in WT controls (Fig. 4C). AO crystalloids, which are typically observed in the peroxisomal matrix of WT cells, were predominantly present inside peroxisomes of *pmp20* cells. Most likely the incorporation of AO in crystalloids prevents bulk leakage of this protein into the cytosol.

Finally, the fate of two key components of the peroxisomal matrix protein import machinery, Pex5p and Pex14p, was analyzed. Western blotting using crude extracts of *pmp20* and WT control cells (Fig. 3D) revealed that the levels of Pex5p and nonphosphorylated Pex14p strongly declined in *pmp20* cells relative to those in WT in the 8- to 12-h interval of cultivation of cells on methanol. In the same time interval Pex11p, a peroxisomal membrane protein involved in organelle proliferation, and the constitutive cytosolic protein Pyc1p remained unaffected, suggesting that the reduction in the levels of Pex5p and nonphosphorylated Pex14p in the absence of Pmp20 is specific.

Oxidative stress in pmp20 cells

Since Prxs are important in preventing cellular damage caused by ROS, we analyzed intracellular ROS levels using the ROS-specific fluorescent probe H_2DCFDA and flow cytometry. In glucose-grown cells (t=0 h) ROS-specific fluorescence was below the limit of detection in both *pmp20* cells and WT controls. Eight hours after the shift of cells to methanol over 15% of the *pmp20* cells showed ROS-specific fluorescence, relative to 0.5% in WT (Fig. 5A). Also at 16 h the ROS levels remained significantly higher in *pmp20* cells. High intracellular ROS species may lead to oxidative damage to proteins (protein carbonylation) and lipids. Analysis of protein carbonylation revealed no significant differences in *pmp20* and WT (data not shown). A general method to analyze oxidative damage of lipids is the measurement of thiobarbituric acid reactive substances (reviewed by [35]). Malondialdehyde (MDA) is an important by-product of lipid peroxidation and reacts with TBARS. The data shown in Fig. 5B revealed that MDA levels were similar in WT and *pmp20* cells grown on glucose and after 8 h of cultivation on methanol. At later stages, however, MDA levels were significantly enhanced in *pmp20* cells relative to those of WT controls.

Next we studied the fatty acid composition of *pmp20* and WT cells. The distribution of saturated and unsaturated lipids was approximately identical in glucose-grown *pmp20* and WT cells (Fig. 5C). However, in cells incubated for 8 h on methanol, palmitic acid (C16:0) had reduced by 30% with a concomitant increase in stearic acid (C18:0) and linoleic acid (C18:2). This shift toward increased content of linoleic acid during extended exposure of cells to methanol was even more pronounced after 16 h of incubation. At that time point, both the degree of unsaturation (unsaturated/saturated fatty acids=3.61) and the chain length distribution (C18/C16=4.46) are markedly enhanced in the mutant compared to WT (3.24 and 3.91, respectively). These data suggest a significant impact of the *PMP20* deletion on fatty acid homeostasis, presumably due to deficiencies in peroxisomal long-chain fatty acid oxidation. The increased content of linoleic acid may render the *pmp20* mutant more susceptible to oxidative damage, as exemplified by the significantly increased content of MDA.

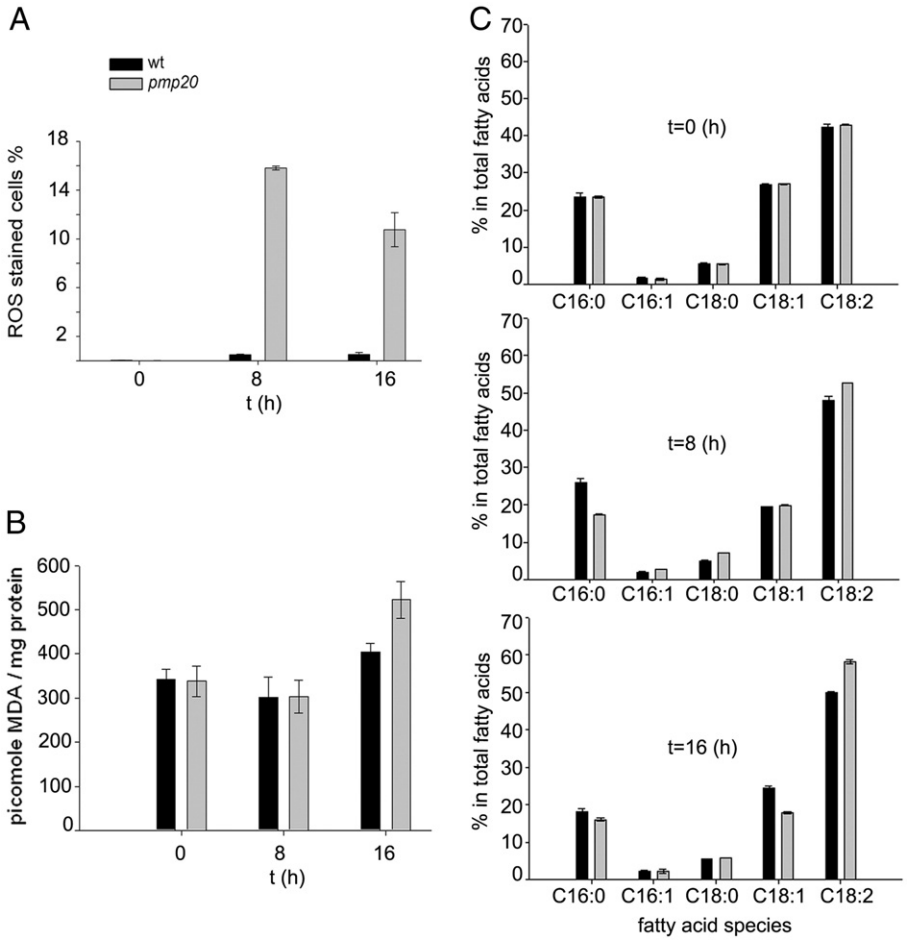

Fig. 5. ROS formation and fatty acid homeostasis. Panel A shows the induction of ROS, determined by flow cytometry of cells incubated with H_2DCFDA. In *pmp20* cells ROS is absent in glucose-grown cells ($t=0$) but strongly induced after 8 or 16 h of growth of *pmp20* cells on methanol. This process is paralleled by enhanced lipid peroxidation in *pmp20* cells after 16 h of cultivation on methanol (B). Oxidative lipid damage is determined by the formation of the by-product malondialdehyde (MDA) after reaction with thiobarbituric acid reactive substances (TBARS). MDA is expressed as picomole/mg protein. Panel C represents the increase in unsaturated fatty acids and chain length distribution in *pmp20* cells after 8 and 16 h of cultivation on methanol. $t=0$ h represent glucose inoculum cells. C16:0 is palmitic acid, C16:1 is palmitoleic acid, C18:0 is stearic acid, C18:1 is oleic acid, C18:2 is linoleic acid. Bars show the percentages of each fatty acid species in total fatty acid amount.

Methanol-induced pmp20 cells show necrotic cell death

Since enhanced intracellular ROS levels may ultimately lead to cell death, we also analyzed whether Pmp20 is important for cell viability. Cell survival was monitored by quantitative analysis of the percentage of colony forming units in a plating assay. As shown in Fig. 6A, the number of colony forming units was similar in *pmp20* and WT cultures after 12 h of incubation in methanol medium. However, after 36 h the *pmp20* cells showed a much lower survival relative to WT controls (Fig. 6A). To test whether this was due to apoptosis, similar studies were performed using a constructed *H. polymorpha PMP20 YCA1* double deletion strain (*pmp20.yca1*). *YCA1* encodes the yeast homologue of mammalian caspase, a protein that plays an important role in apoptosis [36]. *H. polymorpha* Yca1p (NBCI GenBank Accession Number EU543808) was identified by homology search in the *H. polymorpha* genome database using *S. cerevisiae* Yca1p as a bait (63% homology and 52% identity). As shown in Fig. 6A, *yca1* cells showed a similar decrease in viability as WT controls 36 h after the shift to methanol, whereas cultures of the *pmp20yca1* double mutant behaved similar as the *pmp20* single deletion strain. These data indicate that deletion of *YCA1* did not result in suppression of the relatively strong decrease in viability of *pmp20* cultures during incubation in methanol medium.

We finally analyzed markers for apoptosis (Annexin V staining) and necrosis (propidium iodide, PI). Staining of cells with FITC conjugated Annexin V is indicative for externalization of phosphatidylserine, a phenomenon that occurs during early apoptosis [33]. By PI staining the loss of membrane integrity is monitored. Cells that are positively stained with Annexin V, but not with PI, are early apoptotic, whereas late apoptotic cells show both Annexin V and PI staining. Cells that do not stain with Annexin V, but are PI positive, are considered to be necrotic [37].

Fig. 6B shows the quantitative analysis of Annexin V, Annexin V+PI, and PI staining of the four *H. polymorpha* strains (WT, *pmp20, yca1, pmp20yca1*) 36 h after the shift to methanol media. At this time point the percentage of cells stained with PI but not with Annexin V was enhanced in the *pmp20* cultures relative to the WT and *yca1* controls, whereas the percentages of cells stained with Annexin V did not increase. These data are indicative for cell death by necrosis rather than apoptosis. The latter is corroborated by the observation that deletion of *YCA1* in *pmp20* cells did not significantly suppress the increase in percentage of PI-stained cells.

Discussion

Peroxisomal peroxiredoxin is an important antioxidant enzyme

In this study, we analyzed the function of a peroxisomal member of the peroxiredoxin family of antioxidant enzymes, Pmp20, of the yeast *H. polymorpha*. We demonstrate a crucial function of Pmp20 in vivo to prevent protein leakage from the peroxisome and—ultimately—

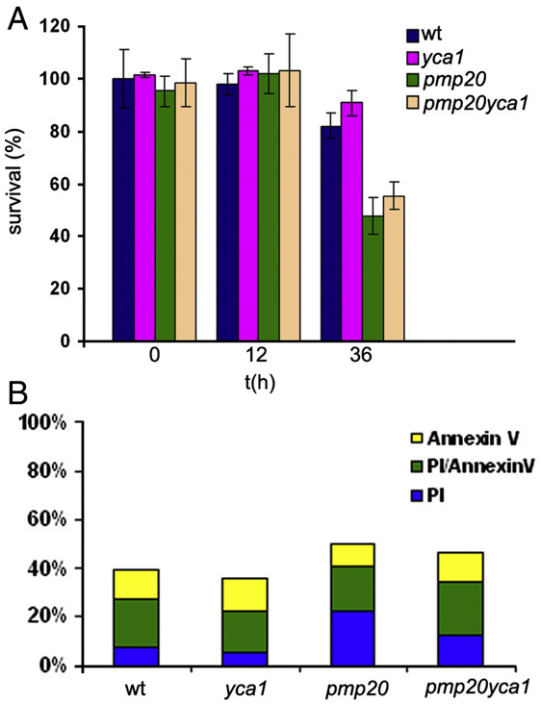

Fig. 6. Survival plating and tests for apoptotic and necrotic markers in wt and *pmp20* cells. Panel A represents cell survival of wt cells and *yca1*, *pmp20*, or *pmp20yca1* mutant cells after the shift to methanol at indicated time points (0, 12, or 36 h). Survival was normalized to wt control at time point 0 (100% survival). Representative experiments are shown, with data representing mean −/+ SEM of 3 independent experiments. Panel B shows quantification of phosphatidylserine externalization and loss of membrane integrity using Annexin V/PI costaining at time point 36 h of the experiment shown in (A). In each experiment, 30,000 cells were evaluated using FACS analysis.

cell death under growth conditions of active peroxisomal oxidative metabolism.

Because of the oxidative character of peroxisomal metabolism, antioxidant enzymes are important in these organelles. Yeast peroxisomes harbor catalase and peroxiredoxins. In higher eukaryotes superoxide dismutase, glutathione peroxidase, or ascorbate peroxidase may occur in peroxisomes as well [2].

Generally, CAT is assumed to play a major role in the decomposition of bulk of the H_2O_2, produced by peroxisomal oxidases. Its importance is stressed by the finding that CAT-deficient *H. polymorpha* strains cannot grow on methanol as sole carbon source [4].

The affinity of CAT for H_2O_2 is, however, rather low (K_m of approx. 25 mM). This, together with the fact that the AO/CAT protein ratio in mature peroxisomes is rather high may result in inefficient H_2O_2 decomposition during growth of cells in the presence of excess methanol. Under these conditions, Prx proteins are required to support growth of *H. polymorpha* on methanol. Prx enzymes are active toward H_2O_2 and alkyl hydroperoxide substrates. In vitro analysis of the properties of *C. boidinii* Pmp20 indicated that this enzyme has a higher affinity for H_2O_2 (K_m of approx. 3 mM) relative to CAT [3].

The affinity of CbPmp20 for alkyl hydroperoxides was in the same range as H_2O_2 (K_m 0.5–1 mM). Hence, Pmp20 may be involved in degrading residual amounts of H_2O_2 as well as in degradation of hydroperoxides. Removal of hydroperoxides from cellular membranes is crucial, because accumulation of these very toxic molecules may further accelerate oxidative decomposition of membrane lipids through radical chain reactions [1,38].

Peroxisomes in pmp20 cells are leaky for proteins

Cells of a constructed *H. polymorpha PMP20* disruption strain (*pmp20*) are defective to sustain growth on methanol, but not on carbon sources that are not metabolized by H_2O_2 generating peroxisomal oxidases (glucose, ethanol, glycerol). Most likely Pmp20 protects peroxisomal membranes against oxidative damage caused by ROS, generated via the H_2O_2 by-product of methanol oxidation. Our combined data suggest that a threshold amount of H_2O_2-producing AO protein must be synthesized to account for the observed deteriorating effects of ROS formation and permeabilization of the peroxisome membrane and, related to this, protein leakage from the organelles. However, peroxisome development is normal in *pmp20* cells and peroxisome membrane disintegration was never observed by electron microscopy. Based on our data we speculate that the peroxisome protein leakage in *pmp20* cells is related to lipid oxidation in the peroxisomal membrane rather than oxidation of peroxisomal membrane proteins. As it is unlikely that proteins can pass a lipid bilayer, changes in the lipid composition most likely influence protein complexes in the peroxisomal membrane, which are ultimately responsible for the observed protein leakage.

Proteins can also release from other cellular organelles. Some of these processes have been well established (e.g., protein export through nuclear pore complexes), whereas the molecular mechanisms behind other export pathways are topic of debate (e.g., the ERAD pathway in the endoplasmic reticulum, the release of proteins from mitochondria at the onset of apoptosis).

Permeabilization of the mitochondrial membrane and release of cytochrome *c* are important processes at the onset of apoptosis. Interestingly, heterologous expression of the human apoptotic inducer Bax in *S. cerevisiae* results in mitochondrial lipid oxidation, which is important for cytochrome *c* release and Bax-mediated cell death [39]. Despite much effort, the principles of Bax-related permeabilization of the mitochondrial outer membrane in yeast and the molecular nature of the mitochondrial apoptosis-induced channel are still unclear (reviewed by [40]). Possibly, the protein permeability changes in peroxisomal membranes of *pmp20* cells have mechanisms in common with this process.

The absence of Pmp20 results in reduced levels of Pex5p and phosphorylated Pex14p

The leakage of peroxisomal matrix proteins into the cytosol coincided with major changes in the levels of Pex5p and Pex14p, two key proteins in PTS1 peroxisomal matrix protein import. Previous data indicated that most likely only nonphosphorylated Pex14p is functional in mediating peroxisomal matrix protein import [41]. Hence, the very low levels of nonphosphorylated Pex14p together with the strongly reduced Pex5p levels in *pmp20* cells will severely affect import of newly synthesized peroxisomal matrix protein import. Therefore, the cytosolic pool of peroxisomal matrix proteins in *pmp20* cells, grown for 16 h in the presence of methanol, most likely represents the added sum of leakage and missorting of newly synthesized peroxisomal matrix proteins.

The observed drop in Pex5p levels may be caused by degradation of the protein by the proteasome. In WT cells, Pex5p is considered to cycle between the cytosol and the peroxisomes [42]. Recycling of Pex5p to the cytosol involves Pex4p-dependent monoubiquination, most likely at a conserved cysteine residue in the N-terminus of Pex5p [43,44]. However, when the Pex5p recycling pathway is blocked (e.g., in *pex4* deletion strains), Pex5p becomes polyubiquitinated and is directed to the proteasome for degradation [45,46]. We speculate that in *pmp20* cells normal recycling of Pex5p may be blocked because of the altered biochemical/biophysical properties of the organelle.

The absence of Pmp20 results in necrotic cell death

Our results suggest for the first time a relationship between the oxidative function of a peroxisomal protein and cell death. In *pmp20*

cultures we observed a decrease in cell survival relative to WT controls. Analysis of apoptosis and necrosis markers revealed that *pmp20* cell death most likely relates to necrosis. This was suggested by the observation that in *pmp20* cultures the percentages of PI-stained cells, indicative for necrosis, were much higher than in the corresponding WT host. Consistently, deletion of gene *YCA1*, encoding a key player in yeast apoptosis, had no major effect on *pmp20*-mediated cell death. Basically, the observed necrosis may be triggered by two distinct or overlapping lipotoxic effects, namely (i) a direct effect as oxidized lipids are known to induce necrosis during atherosclerosis and (ii) an indirect effect related to disturbance of peroxisome function causing enhancement of the intracellular free fatty acid pool and subsequent cell death.

In conclusion, we showed that, in addition to mitochondria, peroxisomes may represent major sites of ROS formation. Our data strongly suggest that the initial deteriorating effects of ROS formation in *H. polymorpha pmp20* cells are confined to peroxisome function and integrity and exert severe effects on cell function and viability.

Acknowledgments

This work was supported by a grant from the Netherlands Organisation for Scientific Research NWO (Earth and Life Sciences) and a short-term EMBO Fellowship to E.B.A. Work in F.M.`s and S.D.K.`s laboratories is supported by SFB Lipotox projects F3012 and F3005 of the Austrian Science Fund, FWF. We thank Kasia Siudeja, Ron Booij, Arjen Krikken, Gabriela Gogg-Fassolter, and Arjo de Boer for technical assistance in various parts of the work and Rhein Biotech GmbH, Duesseldorf, Germany, for access to the *H. polymorpha* genome database.

Appendix A. Supplementary data

Supplementary data associated with this article can be found, in the online version, at doi:10.1016/j.freeradbiomed.2008.07.010. References [47,48] are also cited there.

References

[1] Valko, M.; Leibfritz, D.; Moncol, J.; Cronin, M. T.; Mazur, M.; Telser, J. Free radicals and antioxidants in normal physiological functions and human disease. *Int. J. Biochem. Cell Biol.* **39:**44–84; 2007.
[2] Schrader, M.; Fahimi, H. D. Peroxisomes and oxidative stress. *Biochim. Biophys. Acta* **1763:**1755–1766; 2006.
[3] Horiguchi, H.; Yurimoto, H.; Kato, N.; Sakai, Y. Antioxidant system within yeast peroxisome. Biochemical and physiological characterization of CbPmp20 in the methylotrophic yeast *Candida boidinii*. *J. Biol. Chem.* **276:**14279–14288; 2001.
[4] Verduyn, C.; Giuseppin, M. L.; Scheffers, W. A.; van Dijken, J. P. Hydrogen peroxide metabolism in yeasts. *Appl. Environ. Microbiol* **54:**2086–2090; 1988.
[5] Terlecky, S. R.; Koepke, J. I.; Walton, P. A. Peroxisomes and aging. *Biochim. Biophys. Acta* **1763:**1749–1754; 2006.
[6] van der Klei, I. J.; Yurimoto, H.; Sakai, Y.; Veenhuis, M. The significance of peroxisomes in methanol metabolism in methylotrophic yeast. *Biochim. Biophys. Acta* **1763:**1453–1462; 2006.
[7] Immenschuh, S.; Baumgart-Vogt, E. Peroxiredoxins, oxidative stress, and cell proliferation. *Antioxid. Redox Signal* **7:**768–777; 2005.
[8] Rhee, S. G.; Chae, H. Z.; Kim, K. Peroxiredoxins: a historical overview and speculative preview of novel mechanisms and emerging concepts in cell signaling. *Free Radic. Biol. Med.* **38:**1543–1552; 2005.
[9] Goodman, J. M.; Maher, J.; Silver, P. A.; Pacifico, A.; Sanders, D. The membrane proteins of the methanol-induced peroxisome of *Candida boidinii*. Initial characterization and generation of monoclonal antibodies. *J. Biol. Chem.* **261:**3464–3468; 1986.
[10] Garrard, L. J.; Goodman, J. M. Two genes encode the major membrane-associated protein of methanol-induced peroxisomes from *Candida boidinii*. *J. Biol. Chem.* **264:**13929–13937; 1989.
[11] Yamashita, H.; Avraham, S.; Jiang, S.; London, R.; Van Veldhoven, P. P.; Subramani, S.; Rogers, R. A.; Avraham, H. Characterization of human and murine PMP20 peroxisomal proteins that exhibit antioxidant activity in vitro. *J. Biol. Chem.* **274:**29897–29904; 1999.
[12] Knoops, B.; Clippe, A.; Bogard, C.; Arsalane, K.; Wattiez, R.; Hermans, C.; Duconseille, E.; Falmagne, P.; Bernard, A. Cloning and characterization of AOEB166, a novel mammalian antioxidant enzyme of the peroxiredoxin family. *J. Biol. Chem.* **274:**30451–30458; 1999.
[13] Wang, M. X.; Wei, A.; Yuan, J.; Trickett, A.; Knoops, B.; Murrell, G. A. Expression and regulation of peroxiredoxin 5 in human osteoarthritis. *FEBS Lett.* **531:** 359–362; 2002.
[14] Gérard, A. C.; Many, M. C.; Daumerie, C. h.; Knoops, B.; Colin, I. M. Peroxiredoxin 5 expression in the human thyroid gland. *Thyroid* **15:**205–209; 2005.
[15] Van Dijken, J. P.; Otto, R.; Harder, W. Growth of *Hansenula polymorpha* in a methanol-limited chemostat. Physiological responses due to the involvement of methanol oxidase as a key enzyme in methanol metabolism. *Arch. Microbiol.* **111:** 137–144; 1976.
[16] Waterham, H. R.; Titorenko, V. I.; Swaving, G. J.; Harder, W.; Veenhuis, M. Peroxisomes in the methylotrophic yeast *Hansenula polymorpha* do not necessarily derive from pre-existing organelles. *EMBO J.* **12:**4785–4794; 1993.
[17] Sambrook, J.; Fritsch, E. F.; Maniatis, T. Molecular cloning: a laboratory manual. Cold Spring Harbor Laboratory Press, Cold Spring Harbor, NY; 1989.
[18] Faber, K. N.; Haima, P.; Harder, W.; Veenhuis, M.; AB, G. Highly-efficient electrotransformation of the yeast *Hansenula polymorpha*. *Curr. Genet.* **25:**305–310; 1994.
[19] Merckelbach, A.; Godecke, S.; Janowicz, Z. A.; Hollenberg, C. P. Cloning and sequencing of the ura3 locus of the methylotrophic yeast *Hansenula polymorpha* and its use for the generation of a deletion by gene replacement. *Appl. Microbiol. Biotechnol.* **40:**361–364; 1993.
[20] Ozimek, P.; Lahtchev, K.; Kiel, J. A.; Veenhuis, M.; Van der Klei, I. J. *Hansenula polymorpha* Swi1p and Snf2p are essential for methanol utilisation. *FEMS Yeast Res.* **4:**673–682; 2004.
[21] Haan, G. J.; Faber, K. N.; Baerends, R. J.; Koek, A.; Krikken, A. M.; Kiel, J. A.; van der Klei, I. J.; Veenhuis, M. *Hansenula polymorpha* Pex3p is a peripheral component of the peroxisomal membrane. *J. Biol. Chem.* **277:**26609–26617; 2002.
[22] van der Klei, I. J.; Harder, W.; Veenhuis, M. Methanol metabolism in a peroxisome-deficient mutant of *Hansenula polymorpha*: a physiological study. *Arch. Microbiol.* **156:**15–23; 1991.
[23] Waterham, H. R.; Titorenko, V. I.; Haima, P.; Cregg, J. M.; Harder, W.; Veenhuis, M. The *Hansenula polymorpha PER1* gene is essential for peroxisome biogenesis and encodes a peroxisomal matrix protein with both carboxy- and amino-terminal targeting signals. *J. Cell Biol.* **127:**737–749; 1994.
[24] van der Klei, I. J.; Veenhuis, M.; Nicolay, K.; Harder, W. In vivo inactivation of peroxisomal alcohol oxidase in *Hansenula polymorpha* by KCN is an irreversible process. *Arch. Microbiol.* **151** (1)**:**26–33; 1989.
[25] Keizer, I.; Roggenkamp, R.; Harder, W.; Veenhuis, M. Location of catalase in crystalline peroxisomes of methanol-grown *Hansenula polymorpha*. *FEMS Microbiol. Lett.* **72** (1)**:**7–11; 1992.
[26] van der Klei, I. J.; Hilbrands, R. E.; Swaving, G. J.; Waterham, H. R.; Vrieling, E. G.; Titorenko, V. I.; Cregg, J. M.; Harder, W.; Veenhuis, M. The *Hansenula polymorpha PER3* gene is essential for the import of PTS1 proteins into the peroxisomal matrix. *J. Biol. Chem.* **270** (29)**:**17229–17236; 1995.
[27] Tan, X.; Waterham, H. R.; Veenhuis, M.; Cregg, J. M. The *Hansenula polymorpha PER8* gene encodes a novel peroxisomal integral membrane protein involved in proliferation. *J. Cell Biol.* **128** (3)**:**307–319; 1995.
[28] Komori, M.; Rasmussen, S. W.; Kiel, J. A.; Baerends, R. J.; Cregg, J. M.; van der Klei, I. J.; Veenhuis, M. The *Hansenula polymorpha PEX14* gene encodes a novel peroxisomal membrane protein essential for peroxisome biogenesis. *EMBO J.* **16** (1)**:**44–53; 1997.
[29] Ozimek, P.; van Dijk, R.; Latchev, K.; Gancedo, C.; Wang, D. Y.; van der Klei, I. J.; Veenhuis, M. Pyruvate carboxylase is an essential protein in the assembly of yeast peroxisomal oligomeric alcohol oxidase. *Mol. Biol. Cell.* **14** (2)**:**786–797; 2003.
[30] Bener Aksam, E.; Koek, A.; Kiel, J. A.; Jourdan, S.; Veenhuis, M.; van der Klei, I. J. A peroxisomal lon protease and peroxisome degradation by autophagy play key roles in vitality of *Hansenula polymorpha* cells. *Autophagy* **3:**96–105; 2007.
[31] Buege, J. A.; Aust, S. K. Microsomal lipid peroxidation. *Methods Enzymol.* **52:** 302–310; 1978.
[32] Schneiter, R.; Daum, G. Analysis of yeast lipids. *Methods Mol. Biol.* **313:**75–84; 2006.
[33] Madeo, F.; Fröhlich, E.; Fröhlich, K. U. A yeast mutant showing diagnostic markers of early and late apoptosis. *J. Cell Biol.* **139:**729–734; 1997.
[34] Ramezani-Rad, M.; Hollenberg, C. P.; Lauber, J.; Wedler, H.; Griess, E.; Wagner, C.; Albermann, K.; Hani, J.; Piontek, M.; Dahlems, U.; Gellissen, G. The *Hansenula polymorpha* (strain CBS4732) genome sequencing and analysis. *FEMS Yeast Res.* **4:**207–215; 2003.
[35] Voss, P.; Siems, W. Clinical oxidation parameters of aging. *Free Radic. Res.* **40:** 1339–1349; 2006.
[36] Madeo, F.; Herker, E.; Maldener, C.; Wissing, S.; Lachelt, S.; Herlan, M.; Fehr, M.; Lauber, K.; Sigrist, S. J.; Wesselborg, S.; Frohlich, K. U. A caspase-related protease regulates apoptosis in yeast. *Mol. Cell* **9:**911–917; 2002.
[37] Buttner, S.; Eisenberg, T.; Carmona-Gutierrez, D.; Ruli, D.; Knauer, H.; Ruckenstuhl, C.; Sigrist, C.; Wissing, S.; Kollroser, M.; Frohlich, K. U.; Sigrist, S.; Madeo, F. Endonuclease G regulates budding yeast life and death. *Mol. Cell* **25:**233–246; 2007.
[38] Machlin, L. J.; Bendich, A. Free radical tissue damage: protective role of antioxidant nutrients. *FASEB J.* **1:**441–445; 1987.
[39] Priault, M.; Bessoule, J. J.; Grelaud-Coq, A.; Camougrand, N.; Manon, S. Bax-induced cell death in yeast depends on mitochondrial lipid oxidation. *Eur. J. Biochem.* **269:**5440–5450; 2002.
[40] Eisenberg, T.; Bttner, S.; Kroemer, G.; Madeo, F. The mitochondrial pathway in yeast apoptosis. *Apoptosis* **12:**1011–1023; 2007.
[41] de Vries, B.; Todde, V.; Stevens, P.; Salomons, F.; van der Klei, I. J.; Veenhuis, M. Pex14p is not required for N-starvation induced microautophagy and in catalytic amounts for macropexophagy in *Hansenula polymorpha*. *Autophagy* **2:**183–188; 2006.
[42] van der Klei, I. J.; Hilbrands, R. E.; Kiel, J. A.; Rasmussen, S. W.; Cregg, J. M.; Veenhuis, M. The ubiquitin-conjugating enzyme Pex4p of *Hansenula polymorpha* is required for efficient functioning of the PTS1 import machinery. *EMBO J.* **17:**3608–3618; 1998.

[43] Williams, C.; van den Berg, M.; Sprenger, R. R.; Distel, B. A conserved cysteine is essential for Pex4p-dependent ubiquitination of the peroxisomal import receptor Pex5p. *J. Biol. Chem.* **282:**22534–22543; 2007.
[44] Carvalho, A. F.; Pinto, M. P.; Grou, C. P.; Alencastre, I. S.; Fransen, M.; S-Miranda, C.; Azevedo, J. E. Ubiquitination of mammalian Pex5p, the peroxisomal import receptor. *J. Biol. Chem.* **282:**31267–31272; 2007.
[45] Kiel, J. A.; Otzen, M.; Veenhuis, M.; van der Klei, I. J. Obstruction of polyubiquitination affects PTS1 peroxisomal matrix protein import. *Biochim. Biophys. Acta* **1745:**176–186; 2005.
[46] Platta, H. W.; Erdmann, R. The peroxisomal protein import machinery. *FEBS Lett.* 2811–2819; 2007.
[47] Sudbery, P. E.; Gleeson, M. A.; Veale, R. A.; Ledeboer, A. M.; Zoetmulder, M. C. *Hansenula polymorpha* as a novel yeast system for the expression of heterologous genes. *Biochem. Soc. Trans.* **16:**1081–1083; 1988.
[48] Salomons, F. A.; Kiel, J. A.; Faber, K. N.; Veenhuis, M.; van der Klei, I. J. Overproduction of Pex5p stimulates import of alcohol oxidase and dihydroxyacetone synthase in a *Hansenula polymorpha* Pex14 null mutant. *J. Biol. Chem.* **275:**2603–2611; 2000.